analytical chemistry

Article

pubs.acs.org/ac

Exploiting Enzyme Catalysis in Ultra-Low Ion Strength Media for Impedance Biosensing of Avian Influenza Virus Using a Bare Interdigitated Electrode

Yingchun Fu,[†,⊥] Zachary Callaway,[†] Jacob Lum,[†,‡] Ronghui Wang,[†] Jianhan Lin,[#] and Yanbin Li*[,†,§,∥]

[†]Department of Biological and Agricultural Engineering, University of Arkansas, Fayetteville, Arkansas 72701, United States

[‡]Cell and Molecular Biology Program, University of Arkansas, Fayetteville, Arkansas 72701, United States

[§]Center of Excellence for Poultry Science, University of Arkansas, Fayetteville, Arkansas 72701, United States

[∥]College of Biosystems Engineering and Food Science, Zhejiang University, Hangzhou 310058, China

[⊥]Key Laboratory of Chemical Biology and Traditional Chinese Medicine Research (Ministry of Education of China), Hunan Normal University, Changsha 410081, P. R. China

[#]Modern Precision Agriculture System Integration Research Key Lab of Ministry of Education of China, China Agricultural University, Beijing 100083, China

Supporting Information

ABSTRACT: Enzyme catalysis is broadly used in various fields but generally applied in media with high ion strength. Here, we propose the exploitation of enzymatic catalysis in ultra-low ion strength media to induce ion strength increase for developing a novel impedance biosensing method. Avian influenza virus H5N1, a serious worldwide threat to poultry and human health, was adopted as the analyte. Magnetic beads were modified with H5N1-specific aptamer to capture the H5N1 virus. This was followed by binding concanavalin A (ConA), glucose oxidase (GOx), and Au nanoparticles (AuNPs) to create bionanocomposites through a ConA−glycan interaction. The yielded sandwich complex was transferred to a glucose solution to trigger an enzymatic reaction to produce gluconic acid, which ionized to increase the ion strength of the solution, thus decreasing the impedance on a screen-printed interdigitated array electrode. This method took advantages of the high efficiency of enzymatic catalysis and the high susceptibility of electrochemical impedance on the ion strength and endowed the biosensor with high sensitivity and a detection limit of 8×10^{-4} HAU in 200 μL sample, which was magnitudes lower than that of some analogues based on biosensing methods. Furthermore, the proposed method required only a bare electrode for measurements of ion strength change and had negligible change on the surficial properties of the electrode, though some modification of magnetic beads/Au nanoparticles and the construction of a sandwich complex were still needed. This helped to avoid the drawbacks of commonly used electrode immobilization methods. The merit for this method makes it highly useful and promising for applications. The proposed method may create new possibilities in the broad and well-developed enzymatic catalysis fields and find applications in developing sensitive, rapid, low-cost, and easy-to-operate biosensing and biocatalysis devices.

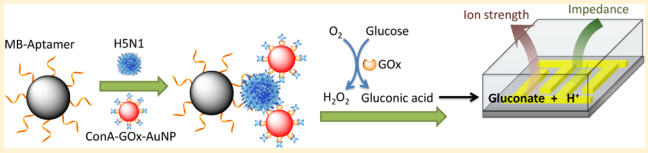

Enzyme catalysis (EC), using enzymes as biological catalysts to catalyze the transformation of substrates with high efficiency and specificity, has drawn a vast amount of research and applications in various academic and industrial fields.[1−5] Although some enzymes have extended their applications in organic and even gas media,[1,3] most enzymes only have activity or high efficiency in aqueous media due to their inherent hydrophilic nature. In aqueous media, ions are generally needed for an efficient enzyme reaction and/or to supply the transformation of substrates or cofactors in some cases. Therefore, buffer solutions and other solutions with high ion strength are generally applied to EC, especially in biorelated systems.[4] However, a high concentration of ions creates a high background for the ion strength-related methods, such as electrochemistry upon the ions (electrolytes). Therefore, introducing EC in media with ultra-low ion strength may provide opportunities to exploit new properties of EC and new applications.

Electrochemical biosensing has become one of the most important research topics in areas including clinic diagnosis/therapy, environmental monitoring, and food safety.[6−12] Novel methods that can develop biosensing devices to fit the sensitive, patchable, low-cost detection in situ are especially important and promising. In these methods, electrode and related immobilization strategies play key roles.[6−12] Although the electrode immobilization strategies are well developed,[6−9] they still suffer from some inherent drawbacks such as (1) sequential immobilization procedures are tedious, complicated, and time

Received: March 12, 2013
Accepted: November 3, 2013
Published: November 3, 2013

Scheme 1. Illustration of the Biosensing Mechanism and Construction of the Biosensor

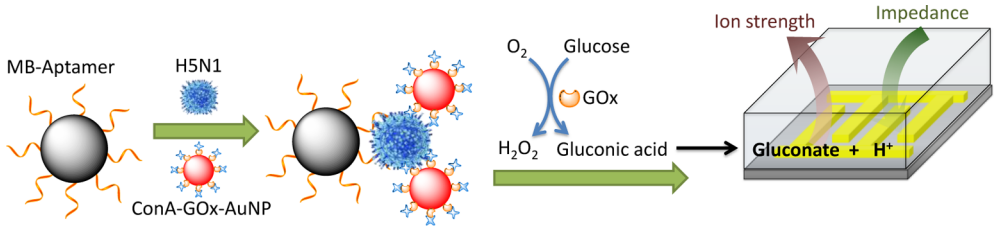

consuming, (2) sensitivity and stability are fragile during transportation and storage, and (3) the reproducibility and regeneration ability are typically low. In contrast, the electrode immobilization-free strategy is highly promising especially for batch and in-field applications.[10,12] However, most of them require a collection of magnetic complexes or other nanomaterials on the surface of the electrode,[10,12] which still makes the electrode difficult to regenerate. Therefore, a new method that can sensitively detect analytes using electrode immobilization-free and easy-to-regenerate electrodes should significantly accelerate the promising applications of biosensing.

Avian influenza viruses (AIV) have attracted global concerns because of the potential pandemic threat for public health, enormous economic losses, and social panic.[13] The highly pathogenic subtype H5N1 virus has caused several devastating out breaks in poultry worldwide.[13] There have been 633 confirmed human cases, with 377 deaths, caused by AIV H5N1 since 2003 according to the report of WHO.[14] Therefore, early, rapid, and sensitive detection and identification of H5N1 is crucial to controlling the outbreaks. Currently, different detection techniques have been developed for AIV detection including virus culture, ELISA, rapid influenza diagnostic test kits, RT-PCR (for some DNA/RNA sequence from the virus), and microarray technology "Flu Chips".[15−23] However, they are either labor intensive, time consuming, require appropriate laboratory facilities and trained technicians, or suffer from low sensitivity and high cost. As an alternative, biosensors have obtained considerable interest for the detection of influenza virus.[24−29] In this lab, a specific aptamer against H5N1 has been successfully screened, and sensitive biosensors using an aptamer and antibody have been developed.[24−26,28,29] However, the present biosensing methods for AIV H5N1 are based on the electrode immobilization manner, which as mentioned above significantly limits their possible applications. Therefore, a simple, rapid, robust, and reliable test, suitable for use in the field or at the patient's bedside, is urgently needed.

Here, we propose the utilization of EC in ultra-low ion strength media to develop an ion strength increase-based impedance biosensor of H5N1 virus on bare electrodes. As illustrated in Scheme 1, streptavidin-coated magnetic beads (MBs) were used to immobilize the biotin-conjugated H5N1 aptamer and then to capture the H5N1 virus. Glucose oxidase (GOx) and concanavalin A (ConA) were sequentially modified onto Au nanoparticles (AuNPs), and these bionanocomposites (BNCs) were conjugated to MB-bound H5N1 through the glycan−ConA interaction. The final complex was transferred to a glucose aqueous solution, where the ion strength was increased through the ionization of the products of EC. Finally, a signal was output detecting the ion strength increase-induced impedance decrease using electrochemical impedance spectroscopy (EIS). A bare screen-printed interdigitated array gold electrode (IDAE) that was designed by this lab was used, as shown in Figure S1 of the Supporting Information. This study elaborated on the EC in ultra-low ion strength media to induce a high susceptibility of electrochemistry upon ions, which was developed as a biosensing method with an ultra-low detection limit. Furthermore, the electrode needed was bare and was only exposed to glucose solutions with different concentrations of gluconic acid, so it was very easy to regenerate for long-term use.

EXPERIMENTAL SECTION

Materials and Apparatus. GOx (EC 1.1.3.4; type II from *Aspergillus niger*, 100−250 kU g^{-1}), glucose, ConA (type VI, from *Canavalia ensiformis* (Jack bean)), $HAuCl_4$, and stock PBS (0.1 M, pH 7.4, containing 1.54 M NaCl) were obtained from Sigma−Aldrich (St. Louis, MO). Stock PBS was diluted at a ratio of 1:10 (10 mM, containing 0.154 M NaCl) and used throughout. Streptavidin-coated magnetic beads with a 150 nm diameter were purchased from R&D Systems, Inc. (Minneapolis, MN). Bovine serum albumin (BSA; EM Science, Gibbstown, NJ), 1.0% (wt/vol), was prepared in PBS as a blocking buffer (PBS BSA). Inactivated AIV H5N1 (128 HAU in PBS solution, HAU means hemagglutination units) was supplied from USDA APHIS Research Laboratory (Ames, IA). The selected aptamer with high affinity and specificity to the AIV H5N1 surface protein was developed in our group, and detailed information on this subject can be found in our previous study.[25,29] Biotin-labeled aptamer was obtained from Integrated DNA Technologies, Inc. (Coralville, IA). The sequences are 5′-biotin-GTGTGCATGGATAGCACGTAACGGTGTAGTAGTAACGTGCGGGTAGGAAGAAAGGGAAATAGTTGTCGTGTTG-3′. All solutions were prepared with deionized water from Millipore (Milli-Q, 18.2 MΩ cm, Bedford, MA).

Impedance measurement was performed using an IM-6 impedance analyzer (BAS, West Lafayette, IN) with IM-6/THALES software. For all impedance measurements, a sine modulated ac potential of 5 mV was applied across the IDAE, and the magnitude of impedance and phase angle were measured for frequencies ranging from 10 Hz to 100 kHz. A DDS-307 conductivity meter with a Pt conductivity probe was used (Rex Instrument Company, Shanghai, China). The IDAE was designed by this lab and produced in Aibit Tech. (Jiangyin, China), as shown in Figure S1 of the Supporting Information. CHI 750b electrochemical workstation (CH Instruments Inc., Austin, TX) and a conventional three-electrode electrolytic cell were used. IDAE served as the working electrode; a KCl-saturated Ag/AgCl electrode served as the reference electrode; and a Pt wire served as the counter electrode. The magnetic separator with a magnetic strength of 0.8 T was provided by Aibit Tech. (Jiangyin, China).

Preparation of ConA/GOx/AuNPs BNCs. AuNPs with a diameter of around 20 nm were prepared through the Frens'

dx.doi.org/10.1021/ac402550f | *Anal. Chem.* 2014, 86, 1965−1971

method.[30] One mL of AuNPs was added to 5 mg of GOx, and then the mixture was rotated at 5 rpm for 1 h and put at 4 °C overnight. After centrifugation and washing with 1 mL PBS twice, the GOx-modified AuNPs were redispersed in 2 mg mL^{-1} of ConA solution in PBS to form the ConA−GOx conjugation through the affinity interaction between ConA and glycan of GOx.[31] The mixture was rotated for 30 min. Finally, the ConA/GOx/AuNPs suspension was centrifuged and washed with PBS twice. The EC activity concentration equaled 0.16 mg mL^{-1} pristine GOx solution. The activity was obtained based on the potentiostatic determination of the amount of enzyme generated H_2O_2, which is proportional to the activity of enzyme,[32] as shown in Figure S2 of the Supporting Information. When not in use, the ConA/GOx/AuNPs BNCs were stored at 4 °C.

Preparation of Sandwich Complex. Ten μL of MBs were added to 200 μL of PBS and magnetically separated for 5 min, and the supernatant was decanted. The MBs were then redispersed in 200 μL of PBS containing 1 μM of a H5N1 biotin−aptamer conjugate and rotated at 5 rpm for 45 min. The solution was then subject to 5 min of magnetic separation, and the supernatant was decanted. Then 200 μL of PBS was added to the MBs along with another 5 min magnetic separation and decantation. The composites were then redispersed in 200 μL of 1% BSA and rotated at 5 rpm for 30 min. This was followed by a 5 min magnetic separation, decantation, and the addition of another 200 μL of PBS for washing. Then after another 5 min magnetic separation and decantation, the composites were redispersed in 200 μL of PBS containing AIV H5N1 at different concentrations (note that all H5N1 mentioned below were used in 200 μL of PBS) and rotated at 5 rpm for 30 min. This was followed by two washing steps involving a 5 min magnetic separation using 200 μL of PBS each time. After the second washing step, the MBs were redispersed in a solution containing 190 μL of PBS and 10 μL of ConA/GOx/AuNPs BNCs and rotated at 5 rpm for 10 min. Because there are about 500 hemagglutinin (HA) and 100 neuraminidase (NA) glycoproteins on the surface of H5N1, the BNCs readily bind to the H5N1 through the ConA−glycan interaction.[33,34] Next, the solution was washed and magnetically separated for 5 min two times using 200 μL of PBS containing 0.05% Tween-20. This was then followed by three washing and 5 min magnetic separation steps using 10 mM of glucose solution. After the last magnetic separation step, the final solution was redispersed in 100 μL of glucose solution. Thirty min later, the suspension was magnetically separated to avoid possible adsorption of sandwich complex on the electrode. The supernatant was transferred to the IDA electrode, and the impedance curve was collected. The impedance value at 1.054 kHz was set as the final signal.

Biosafety Issue. All of testing samples were prepared using inactivated avian influenza virus H5N1 and all tests were conducted in a biosafety level 2 laboratory. Research people were required to get relevant training to conduct the avian influenza tests.

RESULTS AND DISCUSSION

The experimental data of the IDAE in the measurement was represented by an equivalent circuit generated by the IM-6/THALES software, as shown in Figure 1 (top), where C_{di} is the dielectric capacitance, R_s is the bulk solution resistance accounting for change in conductivity of the bulk medium and charge transport across the bulk solution, Z_w is the interfacial impedance (also called Warburg impedance), and C_{dl} is the double layer capacitance accounting for the effect of ionic species on the capacitance near the surface of an electrode.

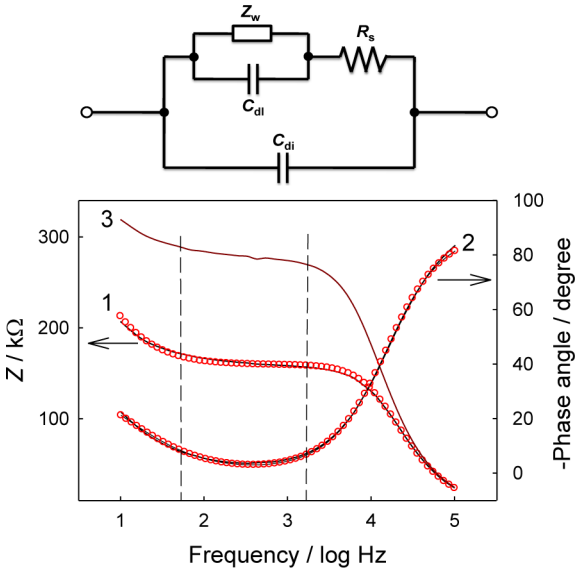

Figure 1. Equivalent circuit (top) and Bode plot (curves 1 and 3 for impedance, curve 2 for phase angle) of the response of the IDAE in 10 mM of glucose solution with (1) and without (2) 5 μM of gluconic acid. The red circle curves are the fitted curves of curves 1 and 2 according to the equivalent circuit.

Figure 1 (bottom) shows the experimental and fitted curve based on the equivalent circuit for the impedance measurement (Bode plot, both magnitude and phase) of the IDAE in 10 mM of glucose solution containing 5 μM of gluconic acid. Curve fitting was performed by the software using a complex nonlinear least-squares method. For comparison, experimental data of a pure 10 mM of glucose solution was also presented. The mean errors of the magnitude of impedance and phase angle were 0.2% and 0.1°, respectively. The largest errors of the magnitude of impedance and phase angle were 2.8% and 2.1°, respectively. This means that this circuit is feasible to simulate the experimental data. There are three critical regions contained in the curves and the equivalent circuit. In the low frequency range from 10 to 60 Hz, the impedance is dominated by the double layer capacitance and the Warburg impedance. The phase angle here showed a trend against 0°. In the frequency range from 60 to 1600 Hz, the impedance remained constant, and the phase angle stayed around 0°, which means the impedance was dominated by the bulk solution resistance (not influenced by frequency). In the frequency range from 1600 Hz to 100 kHz, the impedance had a sharp decrease and the phase angle sharply turned to 90°, which means the dielectric capacitance mainly controls the impedance. The results depict that ion strength is the key factor in determining the bulk solution resistance and thereby the impedance in the middle region. Proof of this has been shown through the experimental and fitted curves from Figure 1 and the significant decrease of impedance compared to the control curve. The largest decrease in impedance was obtained at 1.05 kHz, which was consequently set as the signal readout frequency. Note that although conventional conductivity tests could also provide the solution resistance information, the impedance method provides more detailed information, such as impedance and phase angle values in a large range of frequencies. Furthermore,

dx.doi.org/10.1021/ac402550f | Anal. Chem. 2014, 86, 1965−1971

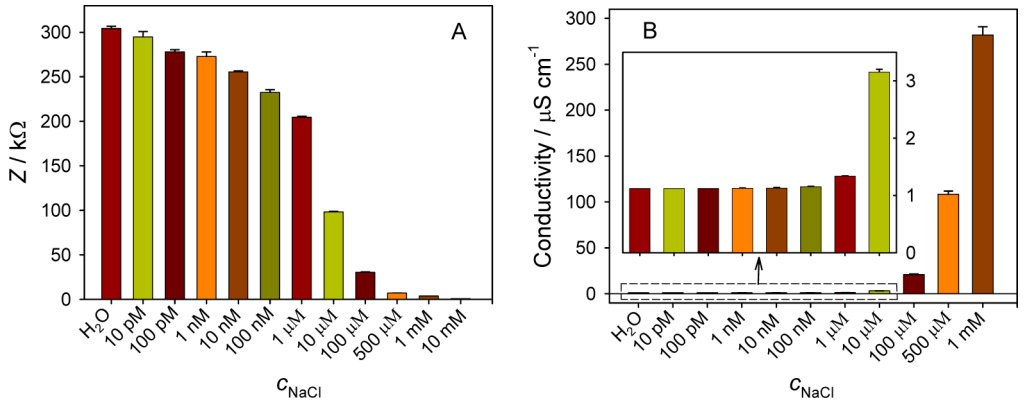

Figure 2. Impedance (A) and conductivity (B) of pure water containing NaCl in different concentrations.

interdigitated array electrodes have advantages in impedance measurement. For example, they can maximize the impedance change at the surface, decrease the detection time, minimize interfering effects of nontarget analytes in the solution, and have high signal/noise ratio.[33,34] These led to the overall decision of using the impedance testing method based on the IDAM for our experimentation.

Considering the high susceptibility of electrochemistry on ion strength, the impedance change from the ion strength increase was estimated by adding an electrolyte, NaCl, as shown in Figure 2(A). We found that the addition of NaCl in water could induce a drastic decrease in impedance. Even ions in concentrations as low as 10 pM NaCl made the impedance decease by 10 kΩ. For comparison, a commercial conductivity meter with a Pt conductivity probe was used to investigate its sensitivity to NaCl concentrations, as shown in Figure 2(B). Conductivity showed an increasing trend along the increase in NaCl concentrations. However, a distinguishable conductivity increase of 4% of that of pure water was found until the NaCl concentration reached 100 nM. This means the proposed method using the IDAE was more sensitive than that using the commercial conductivity meter, though they both are based on the ion strength of the solution. Additionally, the ion strength change in concentrations up to 10 mM NaCl in PBS gave no change in impedance, as shown in Figure S3 of the Supporting Information. This demonstrates that the impedance is highly susceptive to the ion strength change, and the ultra-low ion strength solution is a much better media than the commonly used buffer solution for this experiment.

Because the increase in ionic strength was due to the ionization of gluconic acid produced by GOx catalysis, the dependence of impedance on the concentration of gluconic acid and GOx were also tested, as shown in Figures 3 and 4. We found that 10 mM glucose solution presented ultra-low ion strength, with an impedance (283 kΩ) very close to that of pure water (304 kΩ). This could be explained by the very low pK_a of glucose in water (12.28) and the low diffusion rate of deprotonated glucose. After the addition of gluconic acid solutions, the impedance showed a similar decreasing trend as that of NaCl, with a linear range from 500 nM to 50 μM. The impedance decreased in linear from 21 to 251 kΩ (Figure 3, insert), indicating a large impedance window valuable for the sensitive detection of ion strength change. The minimal concentration was also lower than 100 nM. Considering the p*K*a of gluconic acid (3.86), this minimal concentration of 100 nM was similar to that of NaCl. Furthermore, GOx with different concentrations was also added into 10 mM glucose

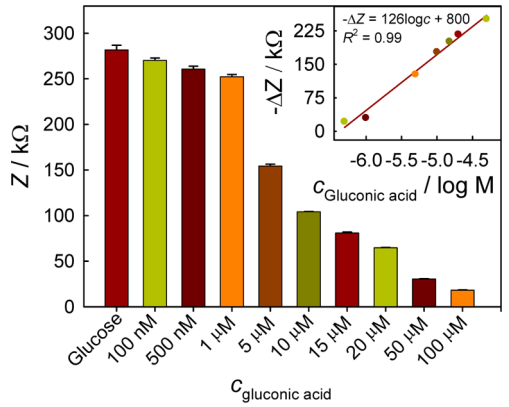

Figure 3. Impedance of 10 mM of glucose solution containing gluconic acid in different concentrations. The insert shows the calibration curve of the means of impedance changes to concentrations of gluconic acid.

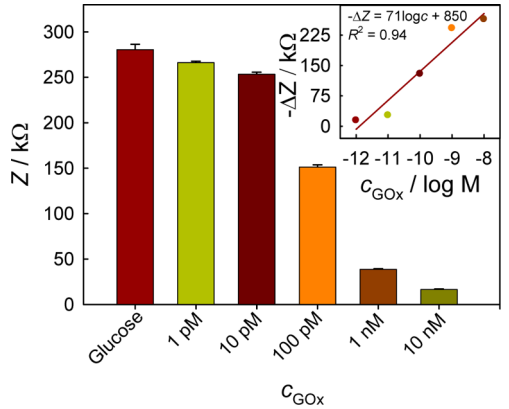

Figure 4. Impedance of 10 mM of glucose solution containing GOx in different concentrations. The insert shows the calibration curve of the means of impedance changes to concentrations of GOx.

solution, and the impedance results were collected after a 30 min reaction, as shown in Figure 4. One can observe that the impedance kept decreasing along with the increase in the concentration of GOx. Even 1 pM of GOx induced an impedance decrease of 14 kΩ, and the linear range extended from 1 pM to 10 nM. When adding 10 nM of GOx, the impedance decreased to only 5.9% of that of a 10 mM of glucose solution. Here, the theory of the high sensitivity of impedance to the GOx catalysis was investigated. The activity

dx.doi.org/10.1021/ac402550f | *Anal. Chem.* 2014, 86, 1965−1971

Table 1. Impedance Changes of Various Electrodes Before and After Immerging in PBS or 10 mM of Glucose Solution

modified electrodes	BSA/apt/strep/Au[a]	H5N1/BSA/apt/strep/Au	BNCs/H5N1/BSA/apt/strep/Au
Z_{change} in PBS (Ω)	−25 ± 19	−47 ± 10	−52 ± 17
Z_{change} in glucose solution (Ω)	−9 ± 4	−22 ± 4	−22 ± 21

[a]apt = aptamer; strep = streptavidin.

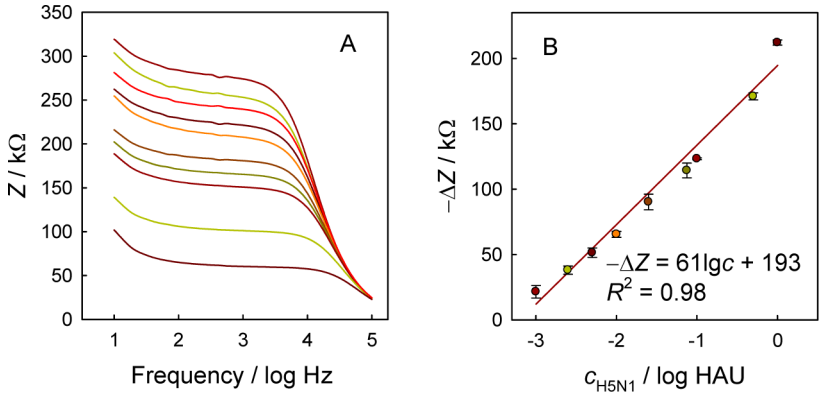

Figure 5. (A) Impedance response curves of biosensors to H5N1 in different concentrations (from top to bottom: control, 0.001, 0.0025, 0.005, 0.01, 0.05, 0.075, 0.1, 0.5, and 1 HAU). (B) Calibration curve and equation.

(100−250 kU g^{-1}) and the definition of a unit (one unit will oxidize 1.0 μmole of β-D-glucose to D-gluconolactone and H_2O_2 per min at pH 5.1 at 35 °C) were provided by the supplier, and we used an estimated average activity of 175 kU g^{-1}. Therefore, the turnover number of GOx in 30 min (N) could be calculated as below

$$N = \frac{A \times 10^{-6}\text{mol}}{\frac{m}{m_w}} \times 30 \quad (1)$$

where A, m, and m_w are the activity (175 kU g^{-1}), mass (1 g), and molecular weight (160 kDa) of GOx, respectively. A number of 8.4×10^5 was used, which means one GOx molecule can catalytically produce 8.4×10^5 gluconic acid molecules in 30 min. This agrees with the minimal concentrations of gluconic acid and GOx to induce an impedance response (100 nM to 1 pM) considering some activity loss of GOx in a low ion strength glucose solution. Therefore, the high sensitivity of impedance to the GOx catalysis in glucose solution should significantly benefit the performance of biosensing and further applications of enzyme catalysis.

Because the sandwich complexes were finally transferred to a 10 mM glucose solution with ultra-low ion strength, the stability of the binding of each recognition pair, including streptavidin−biotin, aptamer−H5N1, and ConA−GOx, were tested. Immobilization procedures were conducted on a streptavidin-modified (physical adsorption) IDAE instead of MBs (BNCs/H5N1/BSA/aptamer/streptavidin/IDAE) to construct a similar sandwich complex on the electrode. After each procedure, the modified electrodes were immerged in PBS or 10 mM glucose solutions for 1 h. EIS in PBS containing 1 mM of $K_3Fe(CN)_4/K_4Fe(CN)_6$ was adopted to investigate and compare the surficial properties before and after the immergence, as listed in Table 1. Surprisingly, modified electrodes immerged in 10 mM of glucose solutions presented much less impedance decrease than that in PBS. Furthermore, an impedance change of −9 ± 18 Ω was achieved using BNC-modified electrodes in a stirred solution of glucose at 200 rpm for 30 min. This means the recognition pairs mentioned above were even more stable in glucose solution than in PBS. The reason might be due to the enhanced interactions between components on the surface of the electrode derived from weakened electrostatic pulses in glucose with a much lower ion strength. Furthermore, the influence of the concentration of glucose on the stability of ConA−GOx and ConA−H5N1 was estimated, and 10 mM of glucose proved to be the favored media considering both EC and stability (see Figure S4, Supporting Information for details). The above results should strongly prove that the sandwich complex in 10 mM of glucose solution was highly stable and show that the complexes did not fall apart during washing and detection.

The impedance response of the biosensors to different concentrations of H5N1 was examined, and the calibration curve was also obtained, as shown in Figure 5. The control experiments showed a blank response of 274 ± 2 kΩ, which was only 9 kΩ lower than that of glucose solution (283 kΩ). This is from the BSA layer on the surface of MBs efficiently blocking the nonspecific adsorption and BSA being a protein that does not bind to ConA.[35,36] The biosensor presented a linear detection range from 0.001 to 1 HAU at log format. The impedance change range was from 21 to 212 kΩ, which was located in the linear range of impedance change to gluconic acid (from 21 to 251 kΩ) and GOx (from 14 to 264 kΩ), demonstrating the reliability of this linear detection range. A detection limit of 8×10^{-4} HAU ($S/N = 3$) was obtained that is magnitudes lower than some other biosensor analogues using antibodies or aptamers that have a detection limits above 0.01 HAU.[24,25,29] Information on this can be found in Table S1 of the Supporting Information. The high performance of this biosensor should mainly be due to the integration of the high efficiency of enzyme catalysis and the high susceptibility of electrochemistry on the ion strength in ultra-low ion strength solution. The performance can also be attributed to the effect of the MB concentration and the introduction of the ConA−glycan interaction to significantly increase the binding sites.

The specificity of this biosensor to other AIVs of different subtypes, including H1N1, H2N2, H5N2, H5N9, and H7N2, has been tested. The impedance responses to 0.5 HAU AIVs of

dx.doi.org/10.1021/ac402550f | Anal. Chem. 2014, 86, 1965−1971

other subtypes were all less than 5% of that to 0.5 HAU H5N1 (Figure S5, Supporting Information), indicating the good specificity of the proposed biosensor. This should be ascribed to the good specificity of the aptamer and also agrees with previous report.[29]

The regenerative ability of the IDAE after multiple detections is a key point for the possible applications of biosensors. Because the EIS method using a redox probe is very powerful for probing the surficial property changes of the electrode surface,[37,38] the surficial properties of IDAE were monitored and compared using EIS in PBS containing 1 mM of $K_3Fe(CN)_4/K_4Fe(CN)_6$. For example, impedance curves were obtained before and after detections more than 50 times per day. The impedance curves were very similar, as shown in Figure S6 of the Supporting Information. This means hundreds of detections had negligible change on the surficial property of the IDAE. Therefore, the proposed method using the detection solution containing only glucose and gluconic acid would have negligible effects on the IDAE surface and to its change in impedance. This means the electrode could be reused over and over without any premodifications, regenerative operations, or excess use of electrode materials and still have very good reproducibility and operation facility. In this experiment, just one IDAE was used throughout all of the related measurements. This merit should make the proposed method quite useful and promising for applications, especially for design of sensitive, rapid, low-cost, and easy-to-operate biosensing devices.

CONCLUSION

In summary, we have exploited EC in ultra-low ion strength media to induce an ion strength increase in the detection of biological analyte using an impedance biosensing method. This method takes advantage of the high efficiency of EC and the high susceptibility of electrochemical impedance on the ion strength and has presented very high sensitivity for the detection of H5N1 assisted by magnetic concentration. The detection limit is down to 8×10^{-4} HAU in a 200 μL sample, which is better than that of some biosensor analogues using antibodies or aptamers. Furthermore, the proposed method just needed a bare electrode for measurements and had negligible change on the surficial properties of the electrode. This helped avoid the drawbacks of commonly used electrode immobilization methods. The merit of this method makes it highly useful and promising for applications, though some modification of magnetic beads/Au nanoparticles and the construction of a sandwich complex were still needed. The proposed method may create new possibilities in the broad and well-developed EC fields and find applications in developing sensitive, rapid, low-cost, and easy-to-operate biosensing and biocatalysis devices.

ASSOCIATED CONTENT

Supporting Information

Additional information as noted in the text. This material is available free of charge via the Internet at http://pubs.acs.org.

AUTHOR INFORMATION

Corresponding Author

*E-mail: yanbinli@uark.edu. Fax: (+) 1 4795752846.

Notes

The authors declare no competing financial interest.

ACKNOWLEDGMENTS

This research was supported in part by the Arkansas Biosciences Institute and National Natural Science Foundation of China (Grant 21105026). The authors thank AIBIT LLC for providing test materials.

REFERENCES

(1) Strohmeier, G. A.; Pichler, H.; May, O.; Gruber-Khadjawi, M. *Chem. Rev.* **2011**, *111*, 4141−4164.
(2) Bornscheuer, U. T.; Huisman, G. W.; Kazlauskas, R. J.; Lutz, S.; Moore, J. C.; Robins, K. *Nature* **2012**, *485*, 185−194.
(3) Klibanov, A. M. *Nature* **2001**, *409*, 241−246.
(4) de laRica, R.; Fratila, R. M.; Szarpak, A.; Huskens, J.; Velders, A. H. *Angew. Chem., Int. Ed.* **2011**, *50*, 5704−5707.
(5) Wang, J. *Chem. Rev.* **2007**, *108*, 814−825.
(6) Xiao, Y.; Lai, R. Y.; Plaxco, K. W. *Nat. Protocols* **2007**, *2*, 2875−2880.
(7) Burke, A. M.; Gorodetsky, A. A. *Nat. Chem.* **2012**, *4*, 595−597.
(8) Cheng, W.; Ding, L.; Ding, S.; Yin, Y.; Ju, H. *Angew. Chem., Int. Ed.* **2009**, *48*, 6465−6468.
(9) Willner, I.; Zayats, M. *Angew. Chem., Int. Ed.* **2007**, *46*, 6408−6418.
(10) Nie, H.; Liu, S.; Yu, R.; Jiang, J. *Angew. Chem., Int. Ed.* **2009**, *48*, 9862−9866.
(11) Fu, Y.; Chen, C.; Xie, Q.; Xu, X.; Zou, C.; Zhou, Q.; Tan, L.; Tang, H.; Zhang, Y.; Yao, S. *Anal. Chem.* **2008**, *80*, 5829−5838.
(12) Fu, Y.; Wang, T.; Bu, L.; Xie, Q.; Li, P.; Chen, J.; Yao, S. *Chem. Commun.* **2011**, *47*, 2637−2639.
(13) Berns, K. I.; Casadevall, A.; Cohen, M. L.; Ehrlich, S. A.; Enquist, L. W.; Fitch, J. P.; Franz, D. R.; Fraser-Liggett, C. M.; Grant, C. M.; Imperiale, M. J.; Kanabrocki, J.; Keim, P. S.; Lemon, S. M.; Levy, S. B.; Lumpkin, J. R.; Miller, J. F.; Murch, R.; Nance, M. E.; Osterholm, M. T.; Relman, D. A.; Roth, J. A.; Vidaver, A. K. *Nature* **2012**, *482*, 153−154.
(14) Eskelinen, A.-P.; Kuzyk, A.; Kaltiaisenaho, T. K.; Timmermans, M. Y.; Nasibulin, A. G.; Kauppinen, E. I.; Törmä, P. *Small* **2011**, *7*, 746−750.
(15) Stamboulian, D.; Bonvehí, P. E.; Nacinovich, F. M.; Cox, N. *Infect. Dis. Clin. North Am.* **2000**, *14*, 141−166.
(16) Boon, A. C. M.; French, A. M. F.; Fleming, D. M.; Zambon, M. C. *J. Med. Virol.* **2001**, *65*, 163−170.
(17) Poehling, K. A.; Griffin, M. R.; Dittus, R. S.; Tang, Y.-W.; Holland, K.; Li, H.; Edwards, K. M. *Pediatrics* **2002**, *110*, 83−88.
(18) Montalto, N. J. *Am. Fam. Physician* **2003**, *67*, 111−118.
(19) Ng, L. F.; Barr, I.; Nguyen, T.; Noor, S. M.; Tan, R. S.; Agathe, L. V.; Gupta, S.; Khalil, H.; To, T. L.; Hassan, S. S.; Ren, E. C. *BMC Infect. Dis.* **2006**, *6*, 40.
(20) Xie, Z.; Pang, Y. S.; Liu, J.; Deng, X.; Tang, X.; Sun, J.; Khan, M. I. *Mol. Cell. Probes* **2006**, *20*, 245−9.
(21) Mehlmann, M.; Dawson, E. D.; Townsend, M. B.; Smagala, J. A.; Moore, C. L.; Smith, C. B.; Cox, N. J.; Kuchta, R. D.; Rowlen, K. L. *J. Clin. Microbiol.* **2006**, *44*, 2857−62.
(22) Liu, R. H.; Lodes, M. J.; Nguyen, T.; Siuda, T.; Slota, M.; Fuji, H. S.; McShea, A. *Anal. Chem.* **2006**, *78*, 4184−4193.
(23) He, Q.; Velumani, S.; Du, Q.; Lim, C. W.; Ng, F. K.; Donis, R.; Kwang, J. *Clinical Vaccine Immunology* **2007**, *14*, 617−23.
(24) Li, D.; Wang, J.; Wang, R.; Li, Y.; Abi-Ghanem, D.; Berghman, L.; Hargis, B.; Lu, H. *Biosens. Bioelectron.* **2011**, *26*, 4146−4154.
(25) Wang, R.; Li, Y. *Biosens. Bioelectron.* **2013**, *42*, 148−155.
(26) Lum, J.; Wang, R.; Lassiter, K.; Srinivasan, B.; Abi-Ghanem, D.; Berghman, L.; Hargis, B.; Tung, S.; Lu, H.; Li, Y. *Biosens. Bioelectron.* **2012**, *38*, 67−73.
(27) Qi, C.; Tian, X.-S.; Chen, S.; Yan, J.-H.; Cao, Z.; Tian, K.-G.; Gao, G. F.; Jin, G. *Biosens. Bioelectron.* **2010**, *25*, 1530−1534.
(28) Wang, R.; Wang, Y.; Lassiter, K.; Li, Y.; Hargis, B.; Tung, S.; Berghman, L.; Bottje, W. *Talanta* **2009**, *79*, 159−164.
(29) Bai, H.; Wang, R.; Hargis, B.; Lu, H.; Li, Y. *Sensors* **2012**, *12*, 12506−12518.

(30) Zhu, T.; Vasilev, K.; Kreiter, M.; Mittler, S.; Knoll, W. *Langmuir* **2003**, *19*, 9518−9525.
(31) Zhou, L.; Jiang, Y.; Gao, J.; Zhao, X.; Ma, L.; Zhou, Q. *Biochem. Eng. J.* **2012**, *69*, 28−31.
(32) Fu, Y.; Li, P.; Xie, Q.; Xu, X.; Lei, L.; Chen, C.; Zou, C.; Deng, W.; Yao, S. *Adv. Funct. Mater.* **2009**, *19*, 1784−1791.
(33) Radke, S. M.; Alocilja, E. C. *Biosens. Bioelectron.* **2005**, *20*, 1662−1667.
(34) Thomas, J. H.; Kim, S. K.; Hesketh, P. J.; Halsall, H. B.; Heineman, W. R. *Anal. Biochem.* **2004**, *328*, 113−122.
(35) Liu, S.; Wang, K.; Du, D.; Sun, Y.; He, L. *Biomacromolecules* **2007**, *8*, 2142−2148.
(36) Wang, Y.; Gildersleeve, J. C.; Basu, A.; Zimmt, M. B. *J. Phys. Chem. B* **2010**, *114*, 14487−14494.
(37) Ensafi, A. A.; Heydari-Bafrooei, E.; Rezaei, B. *Anal. Chem.* **2012**, *85*, 991−997.
(38) Sosnowska, M.; Pieta, P.; Sharma, P. S.; Chitta, R.; Kc, C. B.; Bandi, V.; D'Souza, F.; Kutner, W. *Anal. Chem.* **2013**, *85*, 7454−7461.